Title
AUTOMATIC ACCELERATION AND SPEED CONTROL FOR AN ANALYTIC ULTRACENTRIFUGE

Permalink
https://escholarship.org/uc/item/0bk2k2f7

Authors
Windsor, Alfred A.
Rich, Thomas H.
Doyle, Robert E.
et al.

Publication Date
1966-08-12

UCRL-16982 Rev.

University of California

Ernest O. Lawrence Radiation Laboratory

AUTOMATIC ACCELERATION AND SPEED CONTROL FOR AN ANALYTIC ULTRACENTRIFUGE

Berkeley, California

Submitted to
Review of Scientific Instruments

UCRL-16982 Rev.
Preprint

UNIVERSITY OF CALIFORNIA

Lawrence Radiation Laboratory
Berkeley, California

AEC Contract No. W-7405-eng-48

AUTOMATIC ACCELERATION AND SPEED CONTROL FOR AN ANALYTIC ULTRACENTRIFUGE

Alfred A. Windsor, Thomas H. Rich, Robert E. Doyle,
and Frank T. Lindgren

August 12, 1966

AUTOMATIC ACCELERATION AND SPEED CONTROL FOR AN ANALYTIC ULTRACENTRIFUGE*

Alfred A. Windsor, Thomas H. Rich, Robert E. Doyle,
and Frank T. Lindgren

Donner Laboratory and Donner Pavilion
Lawrence Radiation Laboratory
University of California
Berkeley, California

August 12, 1966

ABSTRACT

A complete profile of automatic acceleration for an analytic ultracentrifuge is established with an electronic speed-control system. Motor current is controlled by a Sola (resonant transformer) resonant current source during acceleration and when the rotor reaches full speed the Sola saturates, forming a constant-voltage regulator. As full speed is approached, a closed-loop system is introduced which compares the frequency of a magnetic-gear-tooth counter to a reference circuit and then applies the error as voltage increments to the drive motor.

To evaluate performance, a computer program was developed to compare manual control with the automated system. Results indicate greater accuracy in the automated system for the integrated $\omega^2 dt$ during the acceleration phase of ultracentrifuge operation, and extremely stable and accurate control of final speed (to within 10 ppm or less).

INTRODUCTION

The conventional analytic ultracentrifuge requires many manual operations which limit its ability to reproduce the runs accurately. In applications to the human lipoprotein spectra, for example, stability during the entire run is particularly important because such macromolecules have molecular weights extending from 10^5 to 10^{11} units.[1] Substantial flotation of these higher molecular weight lipoproteins occurs during the 5 to 6 minutes of acceleration to full speed (52 640 rpm). Therefore, the first schlieren photographs must be taken during the early part of the run, one while the rotor is still accelerating, one when the rotor reaches full speed, and several during a run lasting 64 minutes at full speed.

Some electronic devices were added to make the system more automatic and stable. Faster control of speed was effected by adding the Spinco speed control modification;[2] the modification itself was changed to improve control, and circuits were added to program a cycle of acceleration and photography.

MANUAL ACCELERATION

We used a Spinco model E ultracentrifuge in this study. The standard model of this centrifuge utilizes a synchronous-gear reference.[3] Reproducible acceleration depends on the manual application of a constant motor current (indicated on an ammeter) while the back emf is changing. Consistent manual application is difficult, however, because the operator must simultaneously adjust the current and watch for cell leaks and vacuum loss.

AUTOMATIC ACCELERATION

We have achieved automatic acceleration of a standard model E centrifuge by equipping it with the Spinco electronic speed control modification[2] and by adding circuits which program a cycle of acceleration and photography. The only manual act necessary for such a modified system is pushing a button to start it. (See Fig. 1.) Initially, motor current is raised from 0 to 14A in exactly 0.50 minute by a motor-driven Powerstat (variable autotransformer) and maintained with a Sola (resonant transformer) at the current shown in Fig. 2 until the full-speed loop comes into range. At that time the motor current drops sharply, and the voltage applied to the motor and silicon control rectifiers (SCR) in series is regulated to the appropriate value shown at the top of the curves. The final motor current is determined by the torque required to spin the rotor at full speed in a vacuum of approximately 10^{-3} torr.

Motor current is controlled by the Spinco amplifier and SCR circuit of the electronic-speed-control modification. We did not use the dc tachometer generator (supplied with the modification) for speed control, because its transfer characteristics (including drifts) are inadequate for precision speed control; nonetheless, we did use it to provide overspeed protection. Stability and precision at full operating rotor speed are made possible by a special resonant circuit that supplies the reference for a given speed.

SPEED PARAMETER RELATIONSHIPS

Rotor Speed to Sensor Frequency

Flux linkages between the steel monitor gear and the permanent-magnet tooth-counter coil (Model 3010-A, Electro Products Laboratories, Chicago 48, Ill.) are related to rpm by the number of gear teeth and the step-up ratio between drive motor and rotor shaft. Eighteen teeth divided by the

5-1/3 gear ratio provide 3-3/8 pulses per revolution of the rotor. Therefore, to match a 52 640 rpm speed, the output of the monitor coil was 2961 Hz (cycles per second).

Counting Period to Presentation Accuracy

An automatic presentation and record of rotor speed during the entire period of the run, including acceleration, was provided by a preset counter (Model 5214L, Hewlett Packard, Palo Alto, Calif.) and recorded with a compatible digital recorder (Model 562A, Hewlett Packard, Palo Alto, Calif.). With such an arrangement, continuous visual presentation of rotor speed is available in 4 or 5 digits (Fig. 4), corresponding to counting periods of 1.939 or 19.39 seconds, respectively.

Maximum Loop Gain to Rotor Inertia

Approximately 5 minutes are required to bring a standard two-cell Analytical-D type rotor up-to-speed, whereas 40 minutes are required for it to coast down to a speed of e^{-1} times 52 640 rpm. These periods show the frictional torque to be about one-eighth acceleration torque, and therefore, the closed-loop response is dominated by the inertia of the rotor. In general, one can expect the closed-loop system to be stable for loop gains as high as the ratio of the rotor-time constant to the system-response time. Tests show this maximum stable loop gain to be approximately 5 000, which is more than adequate for our present application.

Speed Stability to Reference Stability

A double series resonant circuit in the frequency comparator provided a "Z" curve transfer characteristic, because the conventional "S" curve circuit had an ambiguous output for large errors. Figure 3 shows the block diagram of the inductance-capacitance reference and comparator. With this arrangement, no external power is required for sensing speed or for generating the error signal. Although speed errors are reduced to several hundred parts per million (ppm) by sensing frequency, preliminary tests indicate the rotor can be locked in-phase with a crystal-controlled oscillator. Thus, a stability of approximately 2 ppm has been repeatedly demonstrated by superimposing a phase detector "S" curve on the output of the frequency comparator. This latter modification may prove to be a most practical solution for ultraprecise control of rotor speeds.

The rotor runs several hundred rpm faster than the final speed as the Spinco modified speed control comes into range. Figure 4 compares the profile of acceleration of the Spinco electronic-speed-control loop with that of our modified system. A Zener diode was added in a minor loop to keep the amplifier in range, and prevent overshoot when the system shifted from a motor-current control to closed-loop control.

Ultracentrifugation to Acceleration Period

In order to accurately determine the area $\omega^2 t$ under the speed-time curves we wrote a computer program in FORTRAN IV. A best-fit curve of the form $\omega^2 = a + bt + ct^2$ was calculated for every set of three points adjacent along the time axis. For each time interval, the regression curves calculated with the interval boundaries used as points were integrated with respect to t, and were evaluated over the interval; then the mean value was taken. The sum of these increments was taken to be the area under the curve during the acceleration phase. The acceleration period could then be expressed as simply $\int_0^{5.70} \omega^2 dt/\omega^2$ up-to-speed (UTS) minutes of equivalent full-speed ultracentrifugation.

RESULTS

Table I presents a comparison between 3.70 and 5.70 minutes of both manual and automatic acceleration, at which time the first and second schlieren pictures, respectively, are taken. At 5.70 minutes of manual acceleration, the ultracentrifuge approximated full speed if a constant current of 14.5A was applied to the drive motor. For automatic acceleration, a more consistent value of both the $\int_0^t \omega^2 dt$ and the rotor speed was reached after 3.70 and 5.70 minutes. Further, the standard deviation of both these parameters is smaller during automatic acceleration than during manual operations, although this is significant only for rpm at $t = 5.70$ minutes ($p < 0.05$, statistical F test).

Figure 5 shows the profile of rotor speed for manual control. An overshoot of several percent occurs at the region between constant acceleration and constant speed, whereas the curve of speed for the closed loop system shown in Fig. 4 shows a smooth transition followed by speed regulation accurate to 10 ppm.

ACKNOWLEDGMENTS

We particularly wish to thank Frank T. Upham, Electronics Department, Lawrence Radiation Laboratory, for his valuable assistance and advice.

FOOTNOTES AND REFERENCES

[*] Work supported by Research Grants 5-R01-HE-01882-11 and 5-R01-HE-02029-11 from the National Heart Institute, Public Health Service, Bethesda, Maryland, and by the U. S. Atomic Energy Commission.

1. Anders Gustafson, Petar Alaupovic, and Robert H. Furman, Biochem. 4, 596, 1965
2. Beckman Instruments, Inc., Technical Bulletin E-TB-013, February, 1965.
3. E. G. Pickels, Machine Design 22, 102, September 1950.

Table I. Comparison of manual and automatic acceleration and speed control.

Run	rpm at 3.70 min		$\int_0^{3.70}\omega^2 dt/\omega^2 \mathrm{UTS}\ dt$ (min)		rpm at 5.70 min		$\int_0^{5.70}\omega^2 dt/\omega^2 \mathrm{UTS}\ dt$ (min)	
	Manual	Automatic	Manual	Automatic	Manual	Automatic	Manual	Automatic
1	33 135	33 900	0.4513	0.4616	51 954	52 100	1.7849	1.8688
2	33 167	33 896	0.4498	0.4591	51 995	52 219	1.7878	1.8796
3	33 064	34 190	0.4475	0.4627	51 861	52 305	1.7723	1.9037
4	33 362	33 902	0.4562	0.4579	52 042	52 149	1.8035	1.8761
5	33 130	34 056	0.4485	0.4619	51 778	52 205	1.7805	1.8890
6	32 879	34 067	0.4442	0.4634	51 524	52 155	1.7529	1.8864
7	33 123	33 971	0.4494	0.4568	51 977	52 172	1.7806	1.8822
8	--	34 063	--	0.4579	--	52 296	--	1.8956
Mean	33 123	34 006	0.4496	0.4602	51 876	52 200	1.7804	1.8852
SD	± 132	± 99	± 0.0034	± 0.0024	± 166	± 67	± 0.0143	± 0.0104

FIGURE LEGENDS

Fig. 1. Block diagram of automatic speed control (above) including rpm profile parameters (below).

Fig. 2. Sola voltage-current-output characteristics as a function of input voltage.

Fig. 3. Block diagram of L-C reference comparator (above); error signal characteristics (below).

Fig. 4. Comparison of acceleration to full speed of Spinco electronic-speed-control loop (Spinco data) with that of our modified system (clamp data) preventing overshoot.

Fig. 5. A graph of speed vs time for manual speed control having a synchronous gear reference.

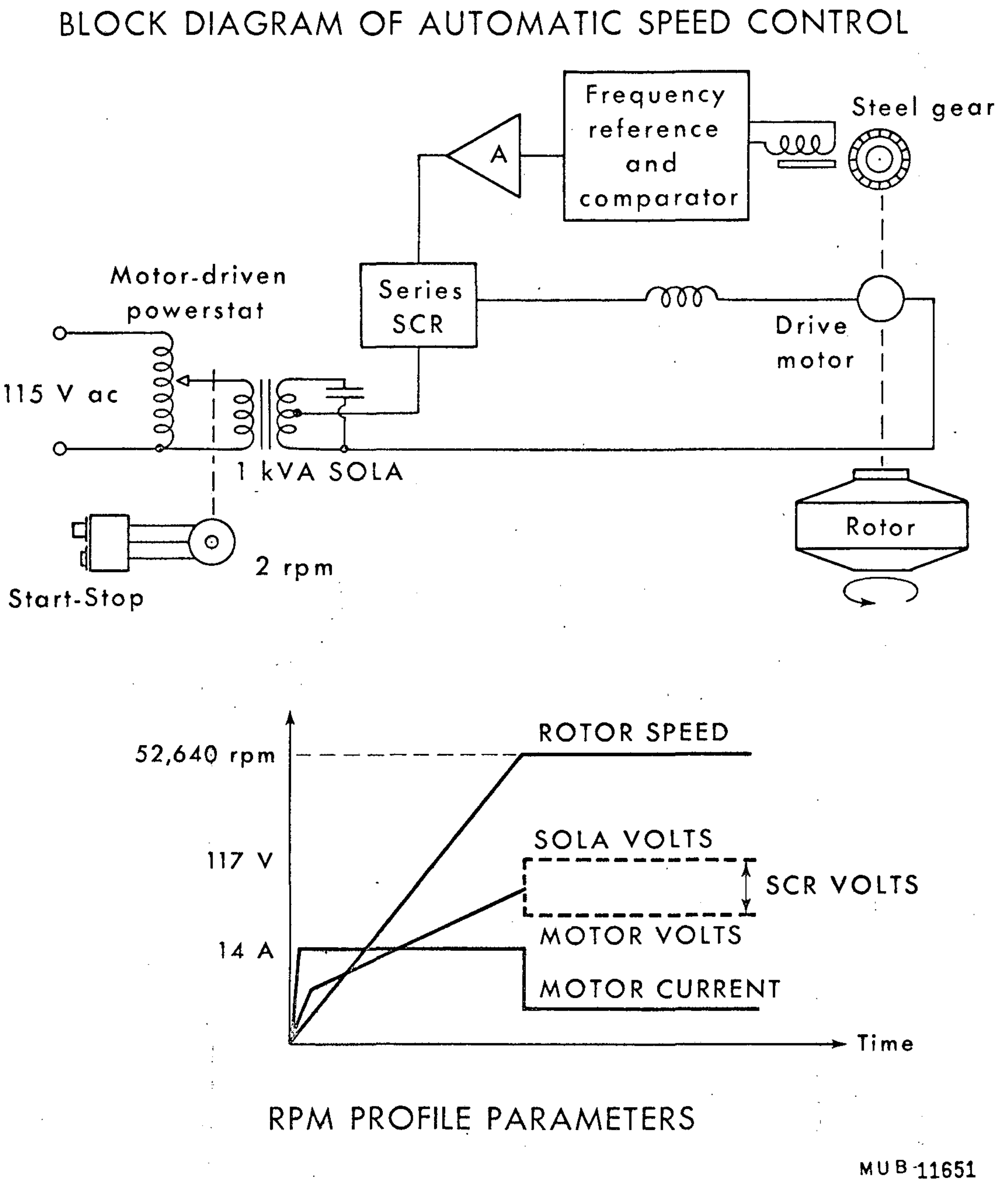

BLOCK DIAGRAM OF AUTOMATIC SPEED CONTROL

RPM PROFILE PARAMETERS

Fig. 1

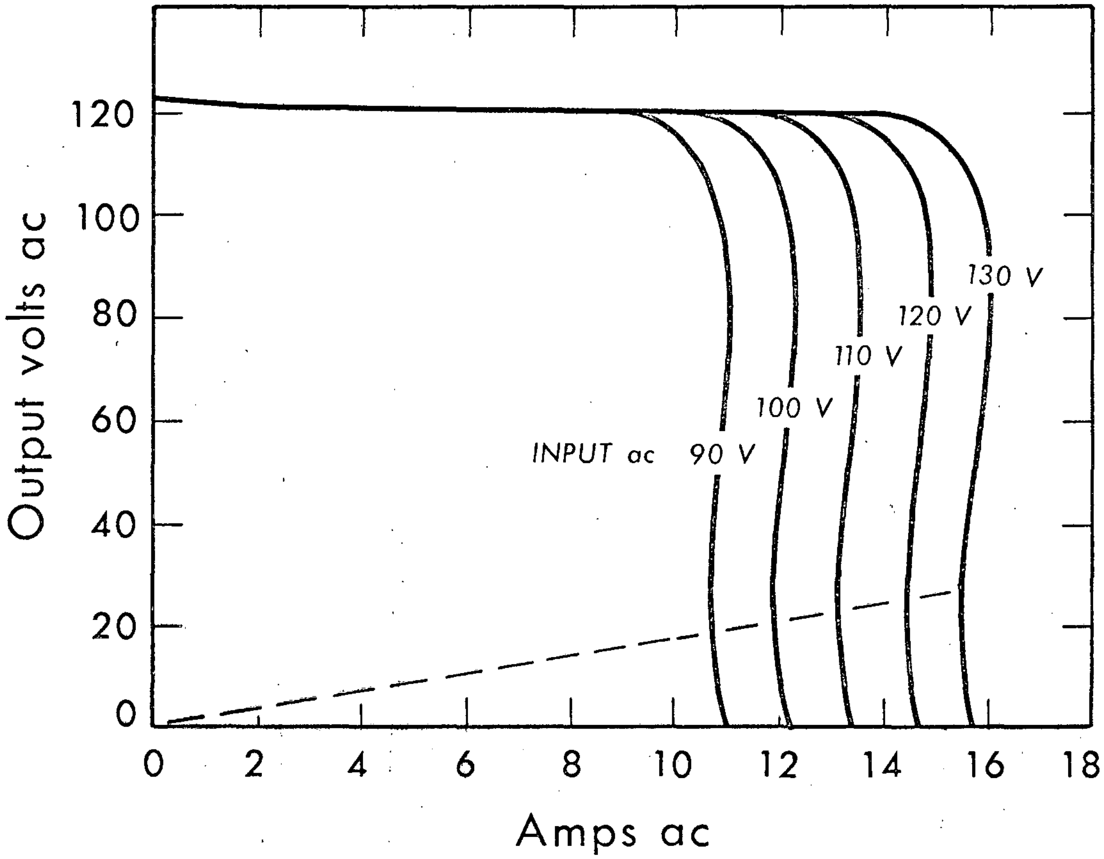

MUB-11650

Fig. 2

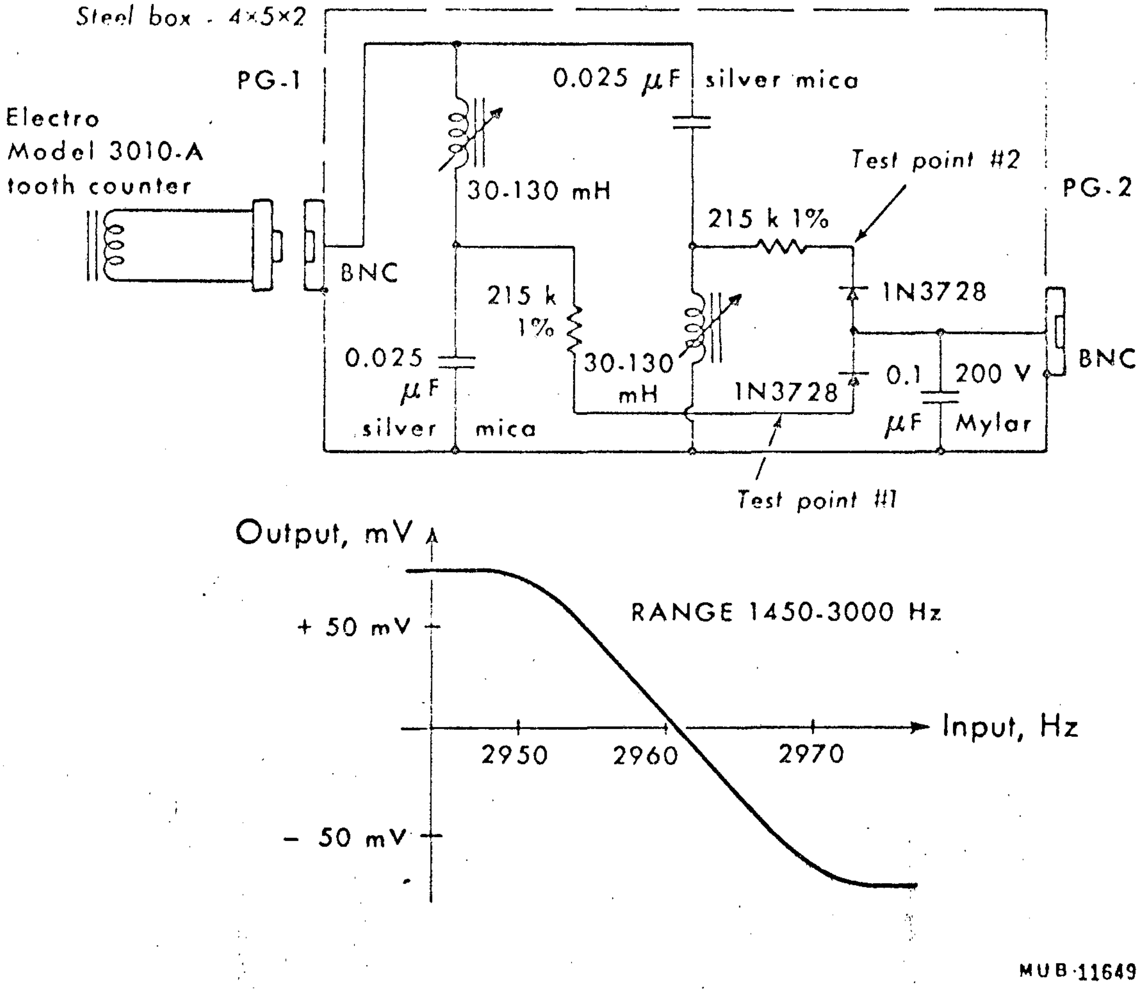
Steel box - 4×5×2
PG-1
Electro
Model 3010-A
tooth counter
BNC
30-130 mH
0.025 μF silver mica
Test point #2
PG-2
215 k 1%
1N3728
215 k
1%
0.025
μF
silver mica
30-130
mH
1N3728
0.1
μF
200 V
Mylar
BNC
Test point #1
Output, mV
+ 50 mV
– 50 mV
RANGE 1450-3000 Hz
Input, Hz
2950
2960
2970
MUB-11649

Fig. 3

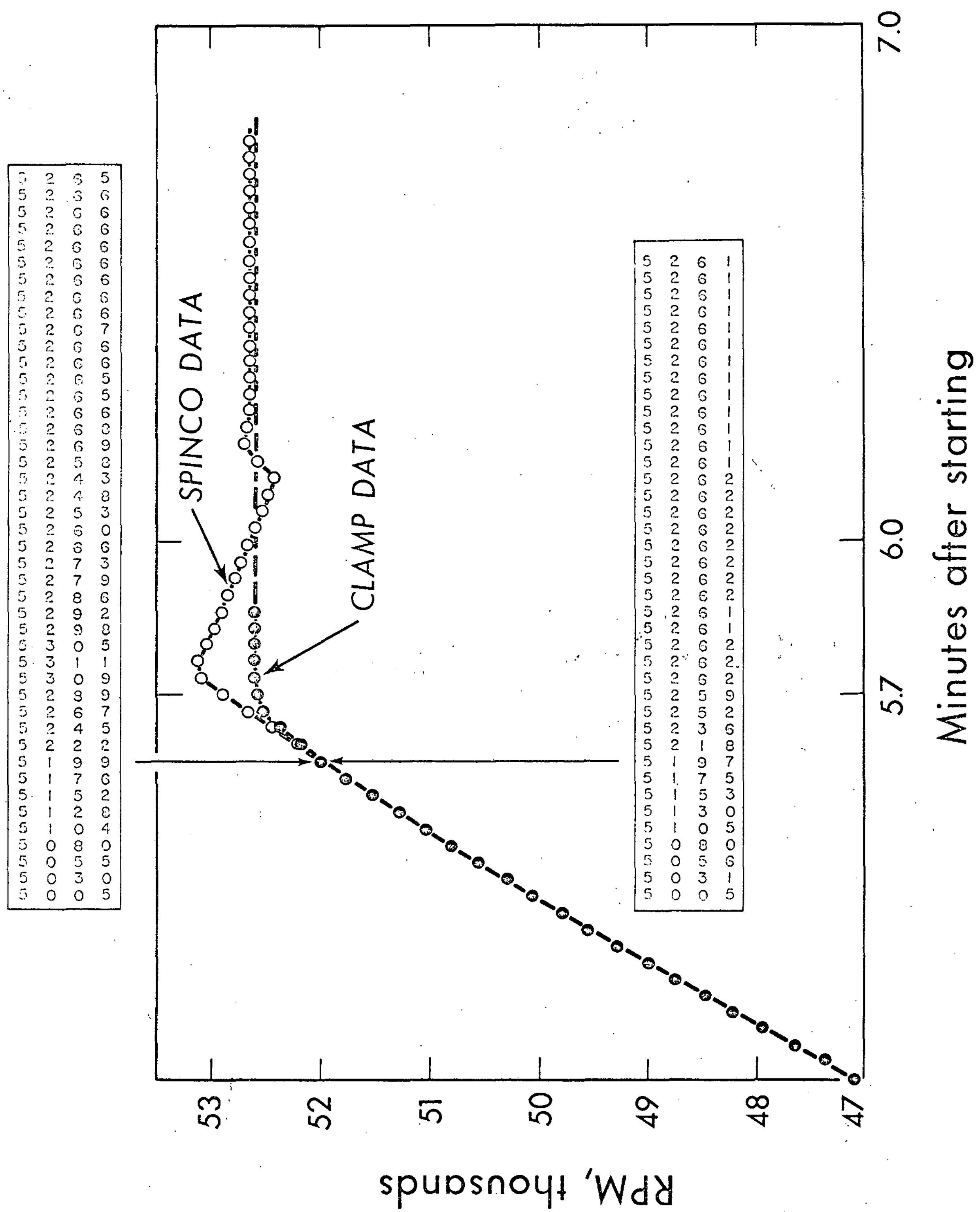

MUB-11652

Fig. 4

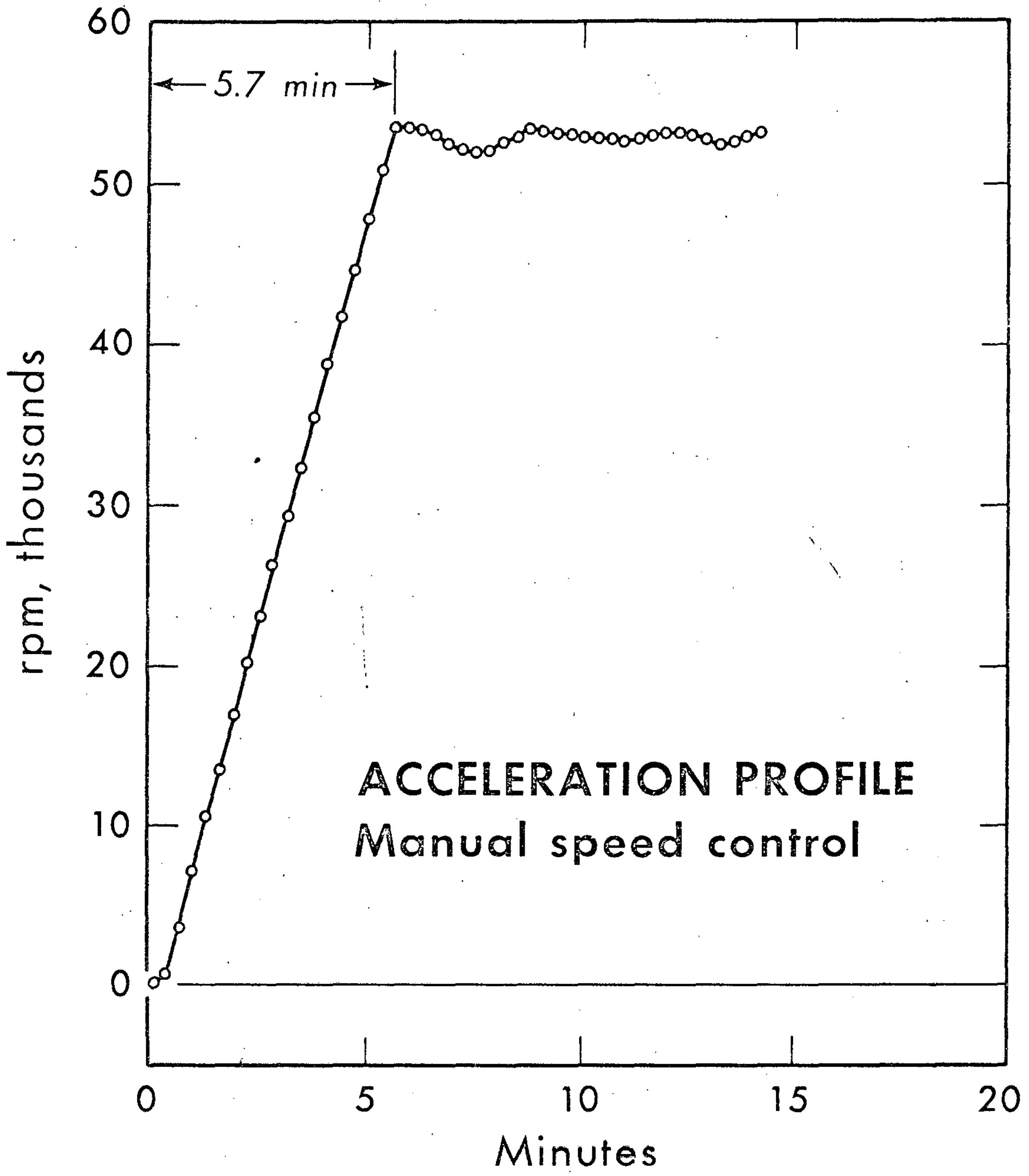

Fig. 5

MUB-11648